PCCP

PAPER

View Article Online
View Journal | View Issue



Cite this: *Phys. Chem. Chem. Phys.*, 2025, **27**, 6104

# Twist-bend liquid crystal phases and molecular structure: the role of methoxybiphenyl†

Calum J. Gibb, ‡*[a] Magdalena M. Majewska,[b] Grant J. Strachan,[b] Damian Pociecha,[b] John M. D. Storey,*[a] Ewa Gorecka[b] and Corrie T. Imrie[a]

Received 23rd October 2024,
Accepted 20th December 2024

DOI: 10.1039/d4cp04076g

rsc.li/pccp

The synthesis and characterisation of the 4-[{[4-({6-[4-(4-methoxyphenyl)phenyl]hexyl}oxy)phenyl]-methylidene}amino]phenyl 4-alkyloxybenzoates is reported. These are referred to using the acronym MeOB6OIBeO*m* in which *m* denotes the number of carbon atoms in the terminal alkyloxy chain and is varied from one to ten. All ten members exhibit an enantiotropic conventional nematic (N) phase. In addition, for *m* = 1–9, the twist-bend nematic ($N_{TB}$) phase was observed on cooling the N phase. The N-isotropic (I) and $N_{TB}$–N transition temperatures decrease on increasing the length of the terminal chain and this is more pronounced for the former. This supports the view that the $N_{TB}$–N transition is predominantly shape driven and this depends largely on the length and parity of the flexible spacer. The transitional behaviour of the MeOB6OIBeO*m* series is compared with that of the corresponding dimers based instead on a cyanobiphenyl fragment, the CB6OIBeO*m* series. The rich smectic polymorphism exhibited by the CB6OIBeO*m* series is extinguished for the MeOB6OIBeO*m* series. The CB6OIBeO*m* series shows higher values of the N–I transition temperature than the corresponding members of the MeOB6OIBeO*m* series whereas the values of the $N_{TB}$–N transition temperatures are rather similar for corresponding members of the two series. This again suggests that the $N_{TB}$–N transition is largely shape driven whereas the mixed core interaction plays a more distinct role in driving N phase formation. The promotion of smectic behaviour in the CB6OIBeO*m* series is attributed to the strong tendency of the cyanobiphenyl fragment to adopt anti-parallel associations.



## Introduction

Reports of spontaneous chiral symmetry breaking in soft matter systems composed of achiral molecules always garner significant attention among the scientific community. The twist-bend nematic ($N_{TB}$) phase provided the first example of such behaviour in a fluid with no positional order.[1–3] First predicted by Meyer[4] and later independently by Dozov[5] a decade before its experimental discovery, in the $N_{TB}$ phase the director adopts a heliconical structure in which it is tilted at an arbitrary angle with respect to the helical axis (Fig. 1(a)). Chirality emerges spontaneously giving doubly degenerate domains of opposite handedness. Molecular chirality removes this degeneracy, and the chiral twist-bend nematic phase is obtained.[6–9] A striking feature of the $N_{TB}$ phase is that the pitch

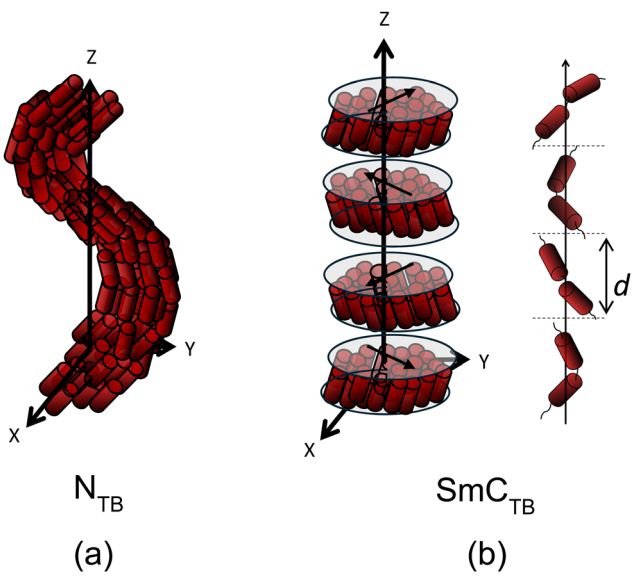


Fig. 1 Sketches of the molecular arrangement in (a) the twist-bend nematic phase ($N_{TB}$) and (b) the twist-bend smectic phase ($SmC_{TB}$).

[a] Department of Chemistry, School of Natural and Computing Sciences, University of Aberdeen, Meston Building, Aberdeen, AB24 3UE, UK. E-mail: c.j.gibb@leeds.ac.uk, j.storey@abdn.ac.uk
[b] University of Warsaw, Faculty of Chemistry, ul. Zwirki i Wigury 101, 02-089, Warsaw, Poland

† Electronic supplementary information (ESI) available. See DOI: https://doi.org/10.1039/d4cp04076g

‡ Current address: School of Chemistry, University of Leeds, Leeds, LS2 9JT, UK.

length of the helix is very short and just a few molecular lengths. At the core of Dozov's prediction was the assumption that bent molecules have a strong natural tendency to pack into bent structures. Such arrangements, however, cannot fill space and so bend must be accompanied by a second deformation, namely twist in the case of the $N_{TB}$ phase. The requirement for a bent molecular structure was realised by using odd-membered liquid crystal dimers and these now constitute the overwhelming majority of the twist-bend nematogens reported to date.[10–16] A liquid crystal dimer consists of molecules containing two semi-rigid mesogenic units, the interactions between which drive the formation of liquid crystal phases, separated by a flexible spacer, most commonly an alkyl chain. The parity of this spacer determines whether the molecules are on average linear or bent.[17]

In his seminal paper, Dozov also predicted the existence of twist-bend smectic phases[5] and these have now also been found, again by studying odd-membered liquid crystal dimers.[18] These have been termed the twist-bend smectic C ($SmC_{TB}$) phases in which the director again forms a heliconical structure having a very short pitch length (Fig. 1(b)).[18] Several structural variants of the $SmC_{TB}$ phase have been discovered[19] although this new class of liquid crystal phase has been observed for rather few molecules, all having similar molecular architectures.[20–23]

The $SmC_{TB}$ phase was first observed in the CB6OIBeO*m* series[18] in which two differing mesogenic units are attached *via* the spacer and this class of materials are referred to as non-symmetric liquid crystal dimers. The CB6OIBeO*m* series contains cyanobiphenyl (CB) and benzylideneaniline benzoate (IBeO) mesogenic units linked *via* a hexyloxy spacer (6O) and *m* represents the number of carbon atoms in the terminal alkyloxy chain (Fig. 2(a)). The CB6OIBeO*m* series displays fascinating liquid crystalline behaviour that depends on the length of the terminal chain (*m*). For terminal chains shorter than the length of the spacer, the $N_{TB}$ phase was observed below the conventional nematic (N) phase. If the terminal chain exceeded the length of the spacer, the $N_{TB}$ phase was extinguished and replaced by a rich smectic polymorphism including the smectic A (SmA), biaxial smectic A ($SmA_b$) and $SmC_{TB\text{-}\alpha}$ phases. Recent studies have further highlighted the importance of the relative lengths of the spacer and terminal chain in determining phase behaviour in this class of materials.[24] We have also shown that the molecular bend angle plays a critical role in determining phase behaviour.[25] Empirically, albeit based on a rather small collection of molecules having similar structures, it appears that the $N_{TB}$ phase is extinguished if the terminal chain length exceeds that of the spacer and twist-bend smectic phases are instead observed.

The driving force for the formation of the smectic phases observed in these materials has recently been suggested to be anti-parallel associations between the benzylideneaniline benzoate mesogenic units and the structure further stabilised by anti-parallel associations between the cyanobiphenyl moieties.[24] In consequence, the smectic mesophases exhibited by these dimers show layer periodicities comparable to full molecular length, $d \sim l$. This contrasts with the behaviour reported for cyanobiphenyl-based non-symmetric dimers containing benzylideneaniline-based units for which the relative lengths of the spacer and terminal chain control the ability of the mesogenic units to interact leading to smectic phases with differing local packing arrangements. For example, for the CBO*n*O*m* series (Fig. 2(b)) when the terminal chain (*m*) is shorter than the spacer (*n*), favourable interactions between the unlike mesogenic groups promote the formation of intercalated structures in which the layer periodicity is approximately half the molecular length, $d \sim l/2$.[26–28] This structure is only stable if the terminal chain can be accommodated in the structural volume determined by the length of the spacer. Increasing the terminal chain destabilises the intercalated arrangements and instead the molecules pack into interdigitated

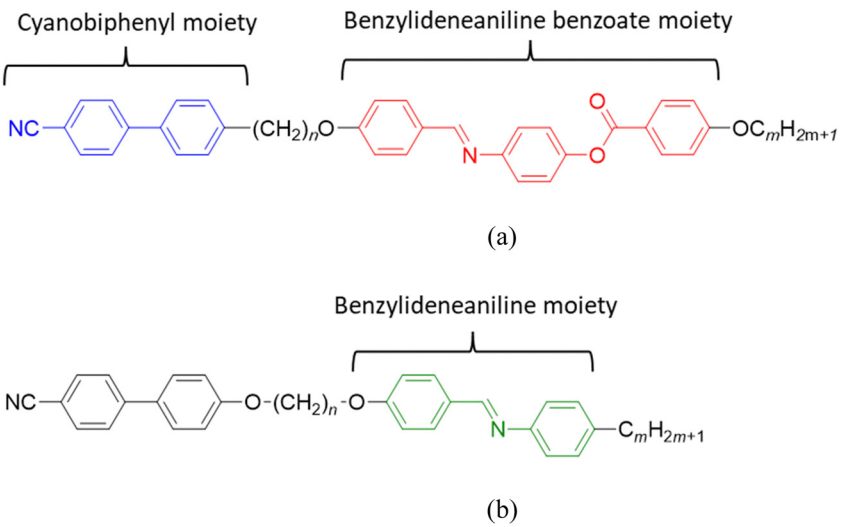


Fig. 2 The general structures of (a) the CB6OIBeO*m* series[18] in which the cyanobiphenyl mesogenic unit is highlighted in blue and the benzylideneaniline benzoate moiety in red, and (b) the CBO*n*O·*m* series[26] in which the benzylideneaniline mesogenic unit is highlighted in green.

structures. These have bilayer periodicities with $d \sim 2l$ and are stabilised by the antiparallel association of the cyanobiphenyl units that serve to minimise dipolar energy while the smectic behaviour is driven by molecular inhomogeneity.[26,27,29]

We have seen that the cyanobiphenyl unit is thought to play an important role in determining the quite different liquid crystal behaviour of the CB6OIBeO*m* (Fig. 2(a))[18] and CBO*n*O*m* series (Fig. 2(b)).[26] Of particular significance is the strong tendency of the cyanobiphenyl group to form anti-parallel associations.[30] To test these suggestions, here we report a series of non-symmetric dimers containing the benzylideneaniline benzoate mesogenic unit but replace the cyanobiphenyl moiety with the methoxybiphenyl mesogenic unit (Fig. 3). We refer to this series using the acronym MeOB6OIBeO*m* series in which MeOB refers to methoxybiphenyl. We selected the methoxybiphenyl unit because it is less polar and polarizable than the cyanobiphenyl moiety and also reduces the structural anisotropy of the molecule. These differences manifest in lower transition temperatures compared to the corresponding cyanobiphenyl-based dimers.[31–33] Critically for this study, the methoxybiphenyl moiety does not show a tendency to exhibit anti-parallel dimers and this should significantly effect the ability of these dimers to exhibit the fascinating smectic phase behaviour seen for the CB6OIBeO*m* series. In terms of molecular design, a hexyloxy spacer was selected to provide the requisite molecular bend for twist-bend phases to be observed.[26,27,29] We compare the transitional properties of the MeOB6OIBeO*m* and CB6OIBeO*m*[18] in order to further understand the role played by molecular structure in determining the fascinating twist-bend phase behaviour.

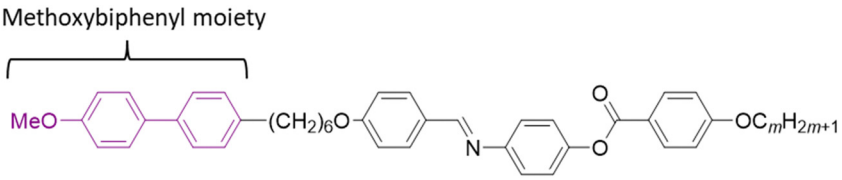


Fig. 3 The general molecular structure of the MeOB6OIBeO*m*, where $m$ = 1–10. The methoxybiphenyl mesogenic unit is highlighted in purple.

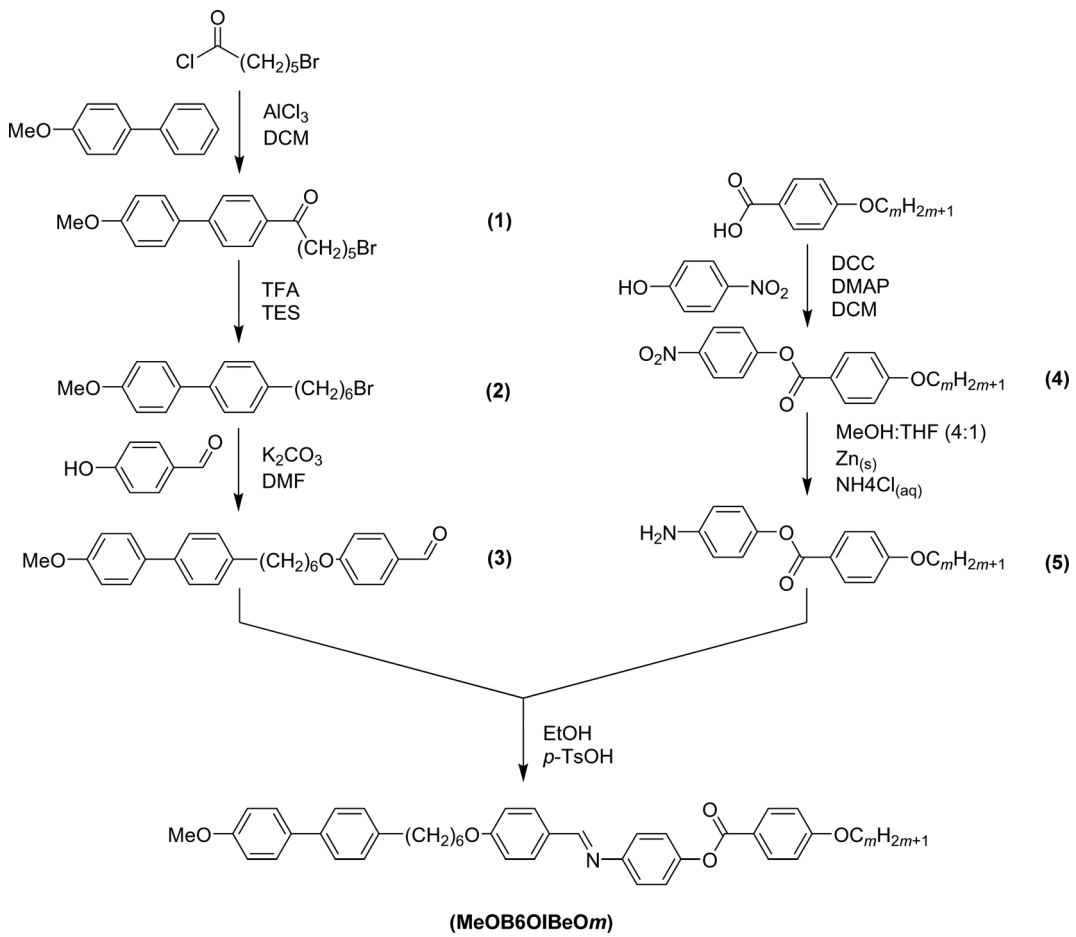


Scheme 1 The synthetic scheme for the synthesis of the MeOB6OIBeO*m* series ($m$ = 1–10).

 

## Experimental

The synthesis of the MeOB6OIBeO*m* series is shown in Scheme 1. The synthesis begins with a Friedel–Crafts acylation reaction between 6-bromohexanoyl chloride and 4-methoxybiphenyl forming 6-bromo-1-(4′-methoxy-[1,1′-biphenyl]-4-yl)hexane-1-one (**1**).[34] The ketone functional group is reduced through treatment with triethyl silane (TEA) and trifluoracetic acid (TFA) forming 4-(6-bromohexyl)-4′-methoxy-1,1′-biphenyl (**2**).[35] A standard Williamson ether synthesis is performed using 4-hydroxybenzaldehyde, generating 4-((6-(4′-methoxy-[1,1′-biphenyl]-4-yl)hexyl)oxy)benzaldehyde (**3**).[33] (**3**) is coupled with the appropriate 4-aminophenyl-4′-alkoxy benzoate ester (**5**)[18,24] using a standard Schiff-base synthesis forming the 4-[{[4-({6-[4-(4-methoxyphenyl)phenyl]hexyl}oxy)phenyl]methylidene}amino]-phenyl 4-alkylbenzoates. Complete synthetic details, along with structural, and purity analysis for the final products and their intermediates are provided in the accompanying ESI.†

Table 1 Transition temperatures (°C) and associated scaled entropy changes for the MeOB6OIBeO*m* series

| | m.p. | | $N_{TB}$–N | | N–I | |
|---|---|---|---|---|---|---|
| *m* | *T*/°C | Δ*S*/*R* | *T*/°C | Δ*S*/*R* | *T*/°C | Δ*S*/*R* |
| 1 | 136.3 | 17.7 | 140.0[a] | ≈0 | 260.2 | 0.44 |
| 2 | 123.3 | 15.7 | 138.5[a] | | 262.2 | 0.54 |
| 3 | 133.8 | 15.8 | 135.5[a] | | 248.6 | 0.38 |
| 4 | 131.4 | 16.1 | 135.0[a] | | 243.0 | 0.38 |
| 5 | 131.0 | 14.1 | 133.0[a] | | 236.5 | 0.35 |
| 6 | 128.4 | 16.0 | 130.0[a] | | 229.7 | 0.36 |
| 7 | 127.9 | 16.9 | [126.5][a] | | 222.0 | 0.34 |
| 8 | 128.1 | 16.9 | [125.5][a] | | 219.3 | 0.34 |
| 9 | 127.2 | 17.0 | [123.0][a] | | 212.8 | 0.28 |
| 10 | 128.2 | 17.6 | — | — | 210.5 | 0.29 |

[a] Microscope observation, [ ] monotropic transition.

## Results and discussion

The transitional properties of the MeOB6OIBeO*m* series are listed in Table 1. All ten members exhibit an enantiotropic nematic phase identified by the observation of Schlieren optical textures containing both 2- and 4-point brush singularities and which flashed when subjected to mechanical stress (Fig. 4(a)). On cooling the N phase for $m$ = 1–9, a blocky, rope-like texture was obtained, characteristic of the $N_{TB}$ phase. The $N_{TB}$ phase was enantiotropic in nature for $m$ = 1–6 and monotropic for 7–9. Representative DSC traces obtained on heating and cooling for MeOB6OIBeO7 are shown in Fig. 4(b). On heating, a strong endotherm associated with the Cr–N transition and a weaker endotherm associated with the N–I transition are observed. The corresponding exotherms are observed in the cooling trace. The $N_{TB}$–N transition is not detected using DSC given that the $N_{TB}$–N phase transition becomes weakly first order as the temperature range of the preceding nematic increases[36] and the MeOB6OIBeO*m* series shows wide temperature range

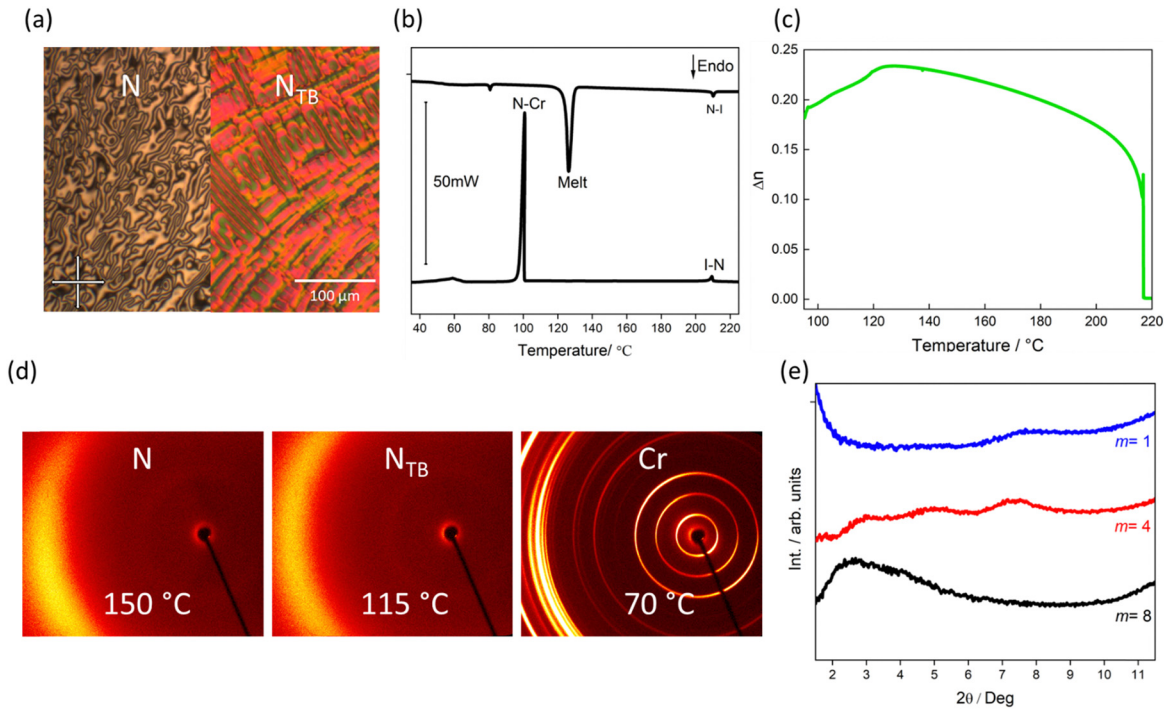


Fig. 4 (a) Characteristic POM textures for a sample sandwiched between untreated glass slides of the N and $N_{TB}$ phases exhibited by MeOB6OIBeO7, (b) DSC thermogram for MeOB6OIBeO9, (c) the temperature dependence of the optical birefringence, $T(\Delta n)$, for MeOB6OIBeO8 measured using green light, $\lambda$ = 532 nm in a 1.7 µm cell treated for planar alignment, (d) 2D X-ray diffraction patterns for MeOB6OIBeO1 in the N [$T$ = 150 °C] (left), $N_{TB}$ [$T$ = 115 °C] (centre) and Cr [$T$ = 70 °C] (right) phases, and (e) the low-angle XRD intensity profiles of the $N_{TB}$ phases shown by homologues with $m$ = 1, 4 and 8 recorded at 115 °C, 128 °C, and 120 °C, respectively, of the MeOB6OIBeO*m* series. The curves have been shifted along the vertical axis for clarity.

nematic phases. Fig. 4(c) shows the temperature dependence of the optical birefringence ($\Delta n$) measured for MeOB6OIBeO8 and a continuous increase in the order parameter is seen on cooling the N phase. At the $N_{TB}$–N transition a characteristic decrease is observed in $\Delta n$ due to the averaging of optical anisotropy resulting from the formation of the short-pitched helix.[37,38]

The phase assignments made using POM for the MeOB6OIBeO*m* series were confirmed using X-ray diffraction (XRD). The diffraction patterns obtained in both the N and $N_{TB}$ phases showed only diffuse scattering in both the small and wide-angle regions indicative of short-range translational ordering (Fig. 4(d)). The local periodicity of the nematic phases may be calculated from the positions of the peak in the small angle region (Fig. 4(e)) and these are given in Table 2. The *d*/*l* ratio for $m = 3$ is approximately 0.33 suggesting an intercalated structure. For $m = 4$ three broad signals are observed corresponding to *d*/*l* ratios of 0.33, 0.50 and 0.84. This suggests a frustrated local structure involving three different packing arrangements. For $m = 8$ a single diffuse peak is again observed with an associated *d*/*l* ratio of 0.84. These data suggest that the local structure in both nematic phases evolves from being intercalated for short terminal chains, experiences frustration for intermediate chain lengths, and adopts an approximately monolayer arrangement for long terminal chain lengths. We note, however, that this change in the local structure cannot be discerned from the dependence of the transition temperatures on *m* (Fig. 5) that shows a regular dependence. Similar behaviour has been reported for the CB6O*m* series.[39] Furthermore, there appears to be no simple relationship between local structure and the helical pitch length in the $N_{TB}$ phase. Both locally bilayer and intercalated types of $N_{TB}$ phases form helical structures with similarly short pitch lengths. The frustration in the local packing mode (as observed, for example, in MeOB6OIBeO9) may be understood as a coexistence of both intercalated and bilayer local structures, but it appears that the breaking of the head and tail equivalence, which is responsible for the bilayer structure, does not affect the formation of the heliconical structure.

Increasing the length of the terminal chain sees essentially a linear decrease in the values of $T_{N-I}$, (Fig. 5), and this may be attributed to the dilution of mesogenic group interactions due to the increasing volume fraction of alkyl chains. The absence of an odd–even effect superimposed on the decreasing trend in $T_{N-I}$ suggests that the effect of the change in molecular shape arising from the disposition of the methyl group with respect to the major axis of the benzylideneaniline benzoate mesogenic unit

Table 2 Molecular end-to-end separation in the N and $N_{TB}$ phases estimated from the position of the small angle peaks in the X-ray patterns, *d*, the estimated molecular lengths, *l*, and the *d*/*l* ratios for selected homologues of the MeOB6OIBeO*m* series

| *m* | *d*/Å | *l*/Å | *d*/*l* |
|---|---|---|---|
| 1 | 11.7 | 39.0 | 0.33 |
| | 12.6 | | 0.33 |
| 4 | 19.3 | 35.5 | 0.50 |
| | 33.0 | | 0.84 |
| 8 | 37.0 | 44.1 | 0.83 |

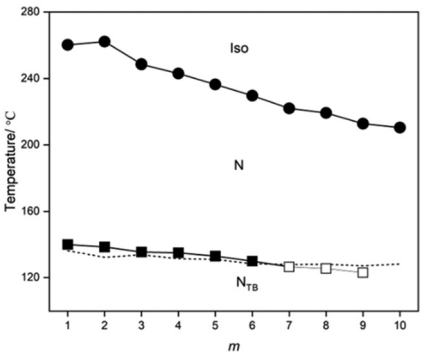


Fig. 5 Temperature dependence of the transition temperatures on increasing terminal chain length (*m*) for the MeOB6OIBeO*m* series. The melting points are indicated by the dotted line. Open symbols represent monotropic phase transition.

on $T_{N-I}$ is much smaller than the dilution effect. The dependence of $T_{N_{TB}-N}$ on *m* is similar but the decrease in $T_{N_{TB}-N}$ on passing from $m = 1$ to 9 is only 17 K whereas that associated with $T_{N-I}$ is 50 K. The smaller change in $T_{N_{TB}-N}$ on increasing terminal chain length suggests that the dilution of interactions between the mesogenic groups has less of an effect on the $N_{TB}$–N transition than on the N–I transition. This is consistent with the view that the formation of the $N_{TB}$ phase is predominantly shape-driven[1,36,40] and that this depends largely on the flexible spacer (Fig. 5).

The phase behaviour of the MeOB6OIBeO*m* series differs dramatically from that of the CB6OIBeO*m* series described earlier.[18] Indeed, the rich smectic polymorphism seen for the latter series is completely extinguished in the former. The $T_{N-I}$

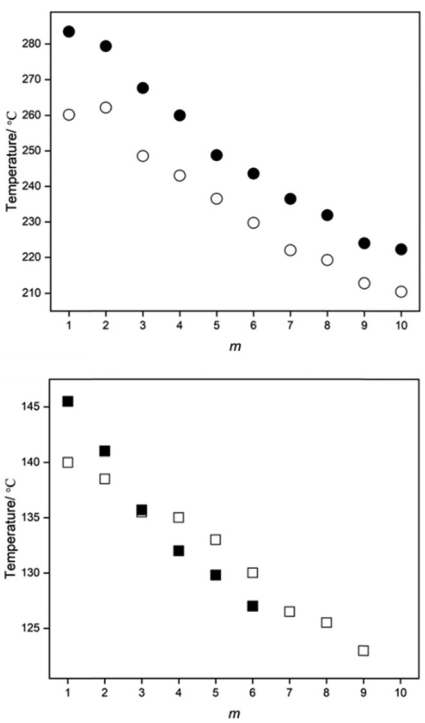


Fig. 6 Comparison of the $T_{N-I}$ [top] and $T_{N_{TB}-N}$ [bottom] for the MeOB6OIBeO*m* [open] and CB6OIBeO*m*[18] [solid] series.

 

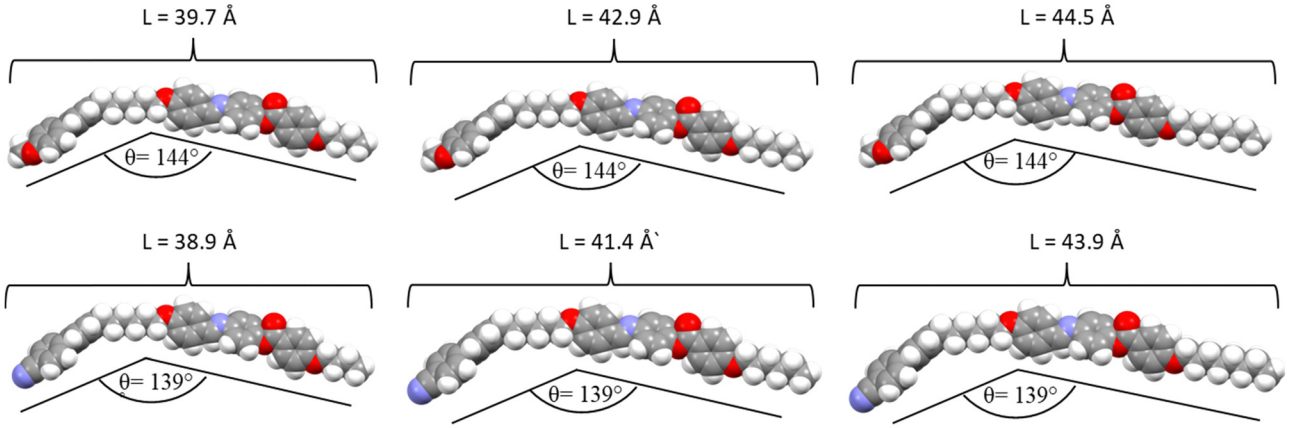


Fig. 7 Geometry optimised structures of the MeOB6OIBeO*m* [top] and CB6OIBeO*m* [bottom] series showing the similarities in molecular structure on increasing the length of the terminal chain (*m*). The structures were obtained by quantum mechanical density functional theory (DFT) calculations at the B3LYP 6-31G(d) level of theory.[41–43]

and $T_{N_{TB}-N}$ transition temperatures for these two series are compared in Fig. 6. As we discussed earlier, replacing a nitrile by a methoxy group reduces $T_{N-I}$ and this is clearly evident in Fig. 6. Over all ten members, $T_{N-I}$ is higher on average by 13.3 K for the CB6OIBeO*m* series. This difference is the largest for the shorter chain lengths and is higher than the difference seen between the CB6O.O*m* and MeOB6O.O*m* series.[33] By comparison, the values of $T_{N_{TB}-N}$ for the two series are very similar and cross-over on increasing *m* (Fig. 6). The larger difference seen for the values of $T_{N-I}$ for these two series may suggest that the interaction between the unlike mesogenic units does play a role in driving nematic phase formation, whereas as we noted earlier the $N_{TB}$–N transition is widely believed to be predominantly shape driven and the shapes of these dimers are rather similar (Fig. 7).

Finally, we consider the absence of smectic behaviour for the MeOB6OIBeO*m* series. The smectic phases exhibited by the CB6OIBeO*m* series are thought to be stabilised by favourable, presumably quadrupolar, interactions between neighbouring pairs of anti-parallel benzylideneaniline benzoate mesogenic units with further stabilisation of the structure coming from anti-parallel associations between the cyanobiphenyl moieties concentrated at the layer interfaces.[24] Methoxybiphenyl fragments do not have the same strong tendency to align in antiparallel associations and this will destabilise the smectic structure. This difference in how the molecular fragments interact results in the observation of the $N_{TB}$ phase for longer terminal chain lengths for the MeOB6OIBeO*m* series compared to the CB6OIBeO*m* series for which the emergent SmA phase precludes the observation of the $N_{TB}$ phase. This contrasting behaviour highlights the importance of the cyanobiphenyl moiety in stabilising the fascinating twist-bend smectic phases.

## Conclusions

We have reported a series of non-symmetric dimers containing methoxybiphenyl and benzylideneaniline benzoate mesogenic units linked by a hexyloxy spacer, the MeOB6OIBeO*m* series. Unlike the corresponding materials containing a cyanobiphenyl moiety,[18] all smectic polymorphism is lost and N and $N_{TB}$ phases are observed across all members of the MeOB6OIBeO*m* series. This dramatic change in phase behaviour is attributed to the importance of anti-parallel associations between the cyanobiphenyl mesogenic units in stabilising lamellar structures in this sub-class of non-symmetric liquid crystal dimers. This observation now has an important role to play in the design of new materials expected to exhibit these fascinating and rare twist-bend liquid crystal phases.

## Data availability

The data supporting this article have been included as part of the ESI.†

## Conflicts of interest

There are no conflicts to declare.

## Acknowledgements

D. P. gratefully acknowledges financial support from the National Science Centre (Poland) under grant no. [2021/43/B/ST5/00240].

## References

1 M. Cestari, E. Frezza, A. Ferrarini and G. R. Luckhurst, *J. Mater. Chem.*, 2011, **21**, 12303–12308.
2 V. Borshch, Y. K. Kim, J. Xiang, M. Gao, A. Jakli and V. P. Panov, *et al.*, *Nat. Commun.*, 2013, **4**, 2635.
3 D. Chen, J. H. Porada, J. B. Hooper, A. Klittnick, Y. Shen and M. R. Tuchband, *et al.*, *Proc. Natl. Acad. Sci. U. S. A.*, 2013, **110**, 15931–15936.

4 R. B. Meyer, Structural problems in liquid crystal physics, Les houches summer school in theoretical physics, in *Molecular Fluids*, ed. R. G. Balian and G. Wil, Gordon and Breach, New York, 1976, pp. 273–373.
5 I. Dozov, *Europhys. Lett.*, 2001, **56**, 247–253.
6 R. Walker, *Liq. Cryst. Today*, 2020, **29**, 2–14.
7 R. Walker, D. Pociecha, J. M. D. Storey, E. Gorecka and C. T. Imrie, *Chem. – Eur. J.*, 2019, **25**, 13329–13335.
8 A. Ozegovic, A. Knezevic, J. Novak, S. Segota, P. Davidson and A. Lesac, *ChemPhysChem*, 2024, **25**, e202400065.
9 A. Ozegovic, J. Hobbs, R. Mandle, A. Lesac and A. Knezevic, *J. Mater. Chem. C*, 2024, **12**, 13985–13993.
10 R. J. Mandle, *Molecules*, 2022, **27**, 2689.
11 R. J. Mandle, *Soft Matter*, 2016, **12**, 7883–7901.
12 E. E. Pocock, R. J. Mandle and J. W. Goodby, *Soft Matter*, 2018, **14**, 2508–2514.
13 P. A. Henderson and C. T. Imrie, *Liq. Cryst.*, 2011, **38**, 1407–1414.
14 N. Tufaha, C. J. Gibb, J. M. D. Storey and C. T. Imrie, *Liq. Cryst.*, 2023, **50**, 1362–1374.
15 G. J. Strachan, M. M. Majewska, D. Pociecha, J. M. D. Storey and C. T. Imrie, *Chem. Phys. Chem.*, 2023, **24**, e202200758.
16 E. Cruickshank, R. Walker, G. J. Strachan, C. H. F. Goode, M. M. Majewska and D. Pociecha, *et al.*, *J. Mol. Liq.*, 2023, **391**, 123226.
17 C. T. Imrie and P. A. Henderson, *Chem. Soc. Rev.*, 2007, **36**, 2096–2124.
18 J. P. Abberley, R. Killah, R. Walker, J. M. D. Storey, C. T. Imrie and M. Salamonczyk, *et al.*, *Nat. Commun.*, 2018, **9**, 228.
19 C. T. Imrie, R. Walker, J. M. D. Storey, E. Gorecka and D. Pociecha, *Crystals*, 2022, **12**, 1245.
20 A. F. Alshammari, D. Pociecha, R. Walker, J. M. D. Storey, E. Gorecka and C. T. Imrie, *Soft Matter*, 2022, **18**, 4679–4688.
21 D. Pociecha, N. Vaupotic, M. Majewska, E. Cruickshank, R. Walker and J. M. D. Storey, *et al.*, *Adv. Mater.*, 2021, **33**, 2103288.
22 A. F. Alshammari, A. Zattarin, A. Pearson, E. Cruickshank, M. Majewska and D. Pociecha, *et al.*, *Liq. Cryst.*, 2024, **51**, 2300–2312.
23 M. Salamonczyk, N. Vaupotic, D. Pociecha, R. Walker, J. M. D. Storey and C. T. Imrie, *et al.*, *Nat. Commun.*, 2019, **10**, 1922.
24 C. J. Gibb, M. Majewska, D. Pociecha, J. M. D. Storey, E. Gorecka and C. T. Imrie, *ChemPhysChem*, 2024, **25**, e202300848.
25 C. J. Gibb, J. M. D. Storey and C. T. Imrie, *Liq. Cryst.*, 2024, **51**, 1956–1963.
26 J. L. Hogan, C. T. Imrie and G. R. Luckhurst, *Liq. Cryst.*, 1988, **3**, 645–650.
27 C. T. Imrie, *Liq. Cryst.*, 2006, **33**, 1449–1454.
28 G. S. Attard, R. W. Date, C. T. Imrie, G. R. Luckhurst, S. J. Roskilly and J. M. Seddon, *et al.*, *Liq. Cryst.*, 1994, **16**, 529–581.
29 A. E. Blatch, I. D. Fletcher and G. R. Luckhurst, *Liq. Cryst.*, 1995, **18**, 801–809.
30 D. A. Dunmur, *Liq. Cryst.*, 2015, **42**, 678–687.
31 J. P. Abberley, J. M. D. Storey and C. T. Imrie, *Liq. Cryst.*, 2019, **46**, 2102–2114.
32 D. A. Paterson, R. Walker, J. P. Abberley, J. Forestier, W. T. A. Harrison and J. M. D. Storey, *et al.*, *Liq. Cryst.*, 2017, **44**, 2060–2078.
33 J. P. Abberley, S. M. Jansze, R. Walker, D. A. Paterson, P. A. Henderson and A. T. M. Marcelis, *et al.*, *Liq. Cryst.*, 2017, **44**, 68–83.
34 D. A. Paterson, M. Gao, Y. K. Kim, A. Jamali, K. L. Finley and B. Robles-Hernández, *et al.*, *Soft Matter*, 2016, **12**, 6827–6840.
35 S. M. Jansze, A. Martínez-Felipe, J. M. D. Storey, A. T. M. Marcelis and C. T. Imrie, *Angew. Chem., Int. Ed.*, 2015, **54**, 643–646.
36 D. A. Paterson, J. P. Abberley, W. T. Harrison, J. M. Storey and C. T. Imrie, *Liq. Cryst.*, 2017, **44**, 127–146.
37 D. Pociecha, C. A. Crawford, D. A. Paterson, J. M. D. Storey, C. T. Imrie and N. Vaupotic, *et al.*, *Phys. Rev. E*, 2018, **98**, 052706.
38 C. Meyer, G. R. Luckhurst and I. Dozov, *J. Mater. Chem. C*, 2015, **3**, 318–328.
39 R. Walker, D. Pociecha, G. J. Strachan, J. M. D. Storey, E. Gorecka and C. T. Imrie, *Soft Matter*, 2019, **15**, 3188–3197.
40 D. A. Paterson, C. A. Crawford, D. Pociecha, R. Walker, J. M. D. Storey and E. Gorecka, *et al.*, *Liq. Cryst.*, 2018, **45**, 2341–2351.
41 M. J. Frisch, G. W. Trucks, H. B. Schlegel, G. E. Scuseria, M. A. Robb, J. R. Cheeseman, *et al.*, *Gaussian 09 (Revision D.01)*, Gaussian Inc., Wallingford CT, 2016.
42 R. Dennington, T. Keith and J. Millam, *Gauss View, Version 5.5*, Semichem Inc, Shawnee Mission, KS, 2009.
43 C. F. Macrae, I. Sovago, S. J. Cottrell, P. T. A. Galek, P. McCabe and E. Pidcock, *et al.*, *J. Appl. Crystallogr.*, 2020, **53**, 226–235.

 